# Identification of Manganese Crusts in 3D Visual Reconstructions to Filter Geo-registered Acoustic Sub-surface Measurements

Umesh Neettiyath*, Takumi Sato*, Mehul Sangekar*, Adrian Bodenmann*,
Blair Thornton*, Tamaki Ura† and Akira Asada*
*Institute of Industrial Science
The University of Tokyo
Email: umesh@iis.u-tokyo.ac.jp
†Center for Socio-Robotic Synthesis
Kyushu Institute of Technology

***Abstract*—The volumetric distribution of cobalt-rich manganese crusts (CRC) is of significant interest for mining and geology. Traditionally studying underwater deposits of CRC involved physical sampling from Remotely Operated Vehicles (ROV) or using dredges. Recently, acoustic measurements of crust thickness have been demonstrated that can give a significantly higher spatial resolution for measurement. The probe makes high resolution measurements of sub-surface reflections to calculate the thickness of the deposit. However, CRC coverage is often not continuous and it is difficult to determine from the acoustic signals alone whether an acoustic signal was measured over CRC or not. The authors propose a method to filter these using visual information (3D colour map of the seafloor) from the same region. After locating the acoustic beam on the seafloor, points around the region are selected. A number of analyses are performed on this point cloud to extract parameters that can reliably discriminate between exposed CRC and other types of seafloor. The proposed method was tested on two areas of seafloor - one which is known to contain crust and one which does not contain crust. These two sets of data were then used to train a Support Vector Machine (SVM) classifier. The trained classifier was then tested with the training sets and a test set containing both crust and non-crust regions to verify if the CRC is being detected reliably. The results were promising; in 85.4% of the cases, the detection was successful. The performance will be verified by using larger sets of data. In our future work, the results can be applied to estimate a volumetric distribution of CRC in the region.**

## I. Introduction

The ocean contains large amounts of mineral deposits. Deposits such as the cobalt-rich manganese crusts (CRC), found around the shoulders of sea-mounts, are potential sources of valuable metals, which are being quickly depleted from land based deposits [1]. Mapping and quantitatively estimating the volumetric distribution of these deposits is, therefore, of interest to geologists, oceanographers, and industry.

Due to the vastness and variance in the geological distribution of these deposits, quantitatively estimating the deposits is a challenging task. Sampling CRC with a Remotely Operated Vehicle (ROV), a dredge or a core drill is the traditional method used to study these deposits. The spatial resolution of data collected regarding the thickness of the deposit layer can be improved significantly by using acoustic techniques, and has been demonstrated by the Institute of Industrial Science of the University of Tokyo [2]. The probe employs a high power acoustic pulse, whose sub-surface reflections are recorded. By extracting the reflections from the interfaces above and below the crust layer, the thickness can be determined if the speed of sound through the deposit is known.

Using the acoustic data alone however, it is often difficult to determine whether a measurement was made over exposed CRC or not, since small inclusions or sharp features of the profile of the seafloor can produce multiple reflections. Knowing the context of the acoustic signal can greatly simplify the subsequent processing and improve the reliability of the measurements.

In order to determine if the measurements were made over exposed CRC, the authors propose to use 3D colour reconstructions of the seafloor to identify acoustic signals that are relevant. The 3D mapping system is included as part of the system conducting surveys to assist the acoustic system and the results are collected simultaneously. By tracing the acoustic beam to the seafloor, the location from which the first reflection occurs can be identified on the 3D map. If this region can be identified as crust, the corresponding acoustic measurement can be taken to be a valid measurement; otherwise, it will be discarded. It is possible for trained human eyes to tell crust regions apart from non-crust regions using features such as texture, colour and edges of the 3D map. The authors tried to automate this process by identifying the modalities of visual data that makes this possible. A machine learning classifier was trained using these modalities as training features, which is then used to predict the reliability of acoustic measurements.

The rest of the paper is organized as follows. Section II describes the system employed to collect data. The details of the algorithm is presented in Section III. Section IV details the implementation and results followed by its discussion in Section V.

## II. System Description

The complete system, shown as mounted on an AUV (Boss-A) in fig. 2, consists of visual and acoustic payload subsystems. The visual system uses a sheet laser, camera and a computer for control and storage of recorded data. The camera

978-0-933957-43-5 

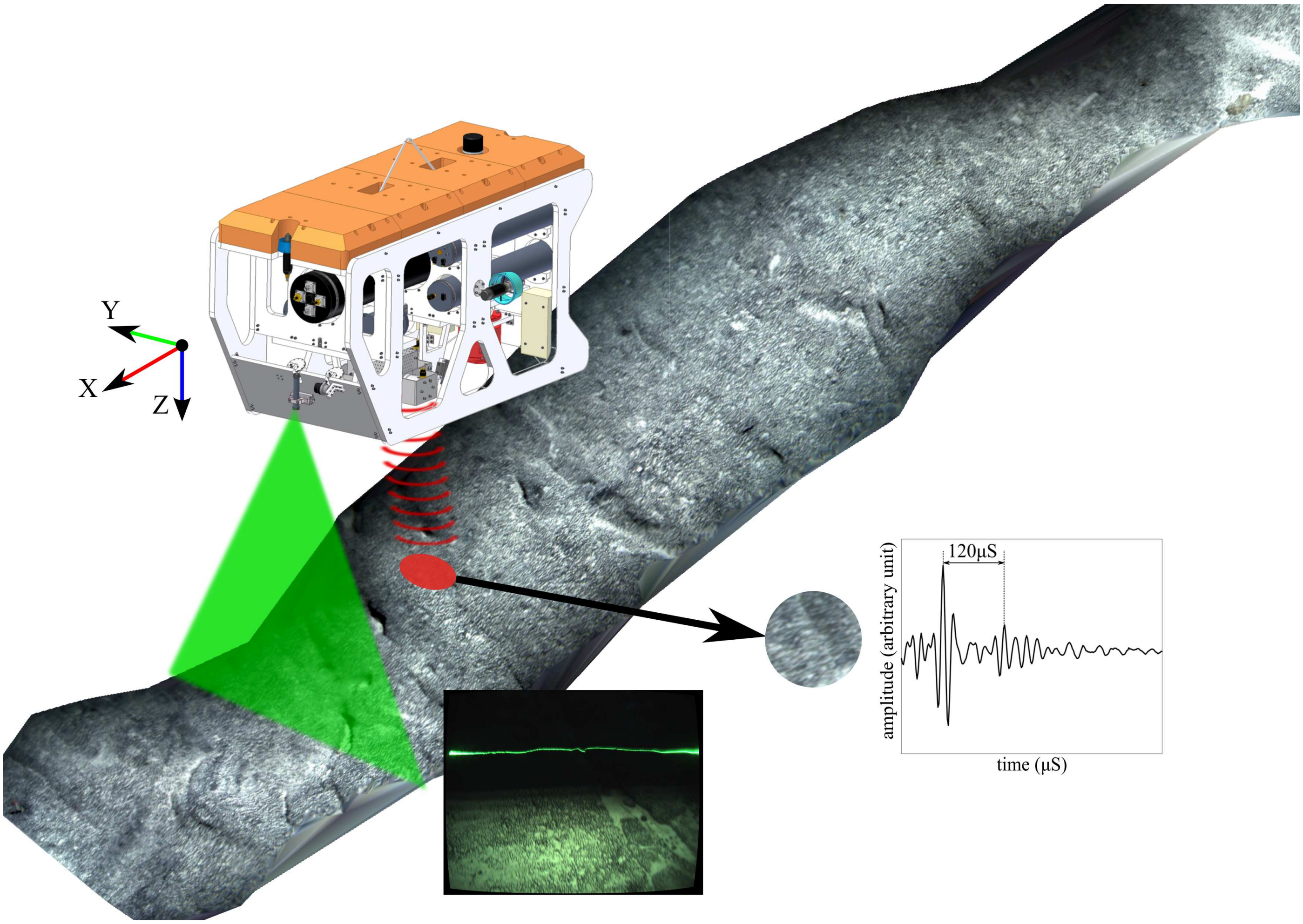


Fig. 1. (System Overview) Visual and acoustic systems, mounted on a robot, surveys a patch of seafloor. On the right is a typical disc of points from the seafloor and a good acoustic reflection from a crust region. Also shown a sample image captured in the camera

records images of the seafloor at a frame rate of (about) 15 frames per second. The 3 dimensional shape of the seafloor is obtained using a structured light technique, in which a laser line is projected onto the seafloor using the sheet laser as illustrated in fig. 1. The projection of the laser line on the seafloor is captured by the offset camera deforms according to the shape of the seafloor. The lower half of the image is illuminated with LED panels; the other half is dark except for the laser line. The colour information of the seafloor is retrieved from the lower half and the shape information is retrieved from the upper half.

The acoustic subsystem is based on a high power probe that is tuned to measure the thickness of the crust layer using acoustic pulses. The probe generates acoustic pulses of frequency 2MHz, amplitude modulated with a signal pulse of 200kHz which generates a parametric wave that penetrates the surface. The system operates at a repetition rate of 20 pulses per second. Accurate measurements require that the pulses hit normal to the seafloor for maximum penetration; i.e, sensor be oriented normal to the seafloor. This is achieved by mounting the probe on a gimballed pan-tilt mount. The desired gimbal orientation is calculated using structured lighting method by calculating the deformation of the laser line on the seafloor

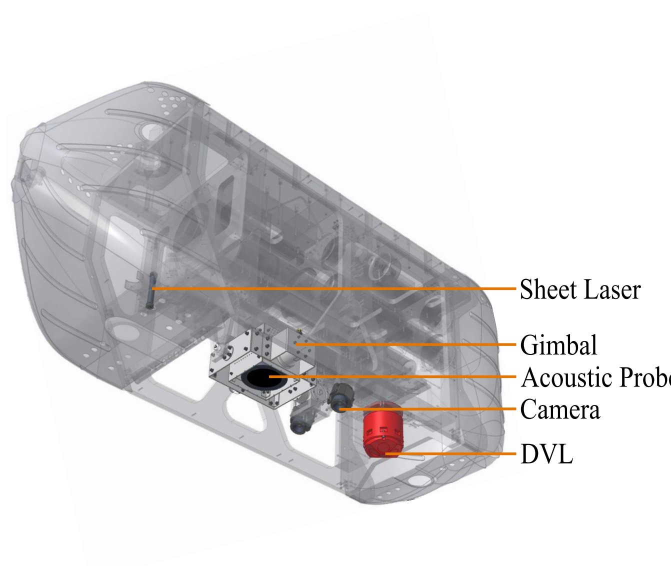


Fig. 2. Components of the acoustic and visual payload systems

together with the height from the seafloor (obtained from DVL) and calculating its orientation; these calculations are done real-time. A separate camera and computer are employed for this purpose. The normal to the surface of the seafloor is calculated from two points on the laser line and the robot's altitude. The gimbal is then oriented along this normal.

Post-processing of the recorded images generates a 3D colour map of the seafloor using the method described in [3]. Similarly, post-processing of the acoustic waves is performed using the method in [2] to calculate a thickness value for each acoustic pulse.

## III. Algorithm and Processing Workflow

After post-processing, the visual system outputs the 3D colour map as a point cloud; each point is characterized by its X,Y, and Z positions in the global coordinate frame and red, green, and blue components of its colour. For a point $i$, these are denoted respectively as $x_i, y_i, z_i, R_i, G_i$, and $B_i$. The acoustic system after post-processing outputs a series of thickness values. Although, they are collected from the same region and simultaneously, the 3D map is about 1.5m wide on average, whereas the thickness value corresponds to a spot of about 2cm in diameter.

Therefore, the first step is to identify the points in the 3D map corresponding to where each ping of the acoustic system hits the seafloor. The position of the probe is denoted as $\eta_{Probe}^{Abs}$ in the global coordinate frame and it may be calculated using equation 1.

$$\eta_{Probe}^{Abs} = \eta_{Robot} + \mathbf{R}\eta_{Probe}^{Rel} \tag{1}$$

where $\eta_{Robot}$ is the position of the robot in the global coordinate frame and $\eta_{Probe}^{Rel}$ is the position of the acoustic probe within the robot. $\mathbf{R}$ is the standard 3 dimensional rotation matrix (Euler Angles system 2) from the local to the global coordinate system, the angles being roll, pitch and yaw of the robot.

After finding the position of the probe and the direction in which it is pointing, a cylinder is defined from the probe along this direction. All points within this cylinder is included into the point cloud and the rest are discarded. This will produce a disc of points, which is used for further processing. The diameter of the cylinder (and hence the generated disc) was set to 10cm, which is higher than the spot diameter of about 2cm in order to minimize the effect of any localization errors. This process is repeated to identify the points of the seafloor that were measured by each ping of the acoustic probe.

Further processing is done on these circular discs of points on the seafloor by assuming that they correspond to the local section of the seafloor where the thickness measurements are taken from. These discs are analyzed to find a number of parameters.

Other parameters calculated directly correspond to or indicate the presence or absence of manganese crusts. Three parameters are calculated in this regard. These are discussed next.

1. Luminosity

The crust deposits are darker in appearance compared to sandy regions. However, this is not immediately identifiable from the point cloud although colour correction is applied to the data, because the luminosity of the generated 3D point cloud can vary based on a number of parameters such as light attenuation with varying height, wavelength dependent colour dispersion in seawater, among others. For each point $i$ the intensity ($I_i$) can be calculated as per equation 2.

$$I_i = 0.21R_i + 0.72G_i + 0.07B_i \tag{2}$$

where $R_i, G_i$ and $B_i$ are the red, green and blue colour values of the point respectively. This will effectively give us a monochrome version of the disc image. The value is averaged over all the points in the disc in order to find the mean value for the entire disc. The standard deviation of luminosity within the disc also show variations between crust and non-crust patches; the crust points show a tendency towards higher values.

2. Entropy

Observing the image of the seafloor indicates that crust regions have a less uniform texture on the scale of the defined disc than the sediment regions. This can be effectively represented by entropy, which is defined as the measure of randomness of an image. Entropy ($E$) can be calculated from the luminous intensity map using equation 3

$$E = -\sum_j P(I_j)\log(P(I_j)) \tag{3}$$

where $P(I_j)$ is the probability that a random point will have a luminous intensity $j$.

3. Altitude angle of seafloor

Analyzing long patches of seafloor showed that large portions of continuous crust deposits occur along the edges or sloping regions of the seamount, whereas sediment regions are mostly along the flat regions. Altitude angle (also called elevation angle in astronomy), which denotes the orientation of the (normal of the) seafloor w.r.t. the zenith (-Z axis of global coordinate frame), is chosen as the parameter to represent this. Equation 4 is used to calculate the altitude angle ($\theta_{alt}$).

$$\theta_{alt} = 90 - \cos^{-1}(\mathbf{N} \cdot \mathbf{V}) \tag{4}$$

A combination of the above parameters can be used to discriminate CRC from other types of seafloor. In order to efficiently and easily perform this classification, a Support Vector Machine (SVM) is used with these parameters as features.

Two classes are defined for this purpose - one for crust and one for everything which is not crust. Before using an SVM for classification, it was be trained with known data. Once trained, it was used to predict the presence of crust for the remaining discs. Once predicted, this can be used to filter the thickness information, which is the output of the acoustic system. The thickness values are kept wherever crust was confirmed and ignored for all other types of seafloor.

## IV. Implementation and Results

Data collected during the NT13-13 research cruise by JAMSTEC using the research vessel Natsushima was used

TABLE I. NAMING OF PATCHES OF SEAFLOOR USED IN THIS PAPER

| Patch No. | Type | Length (m) | No. of Acoustic Measurements | | | Purpose |
|---|---|---|---|---|---|---|
| | | | Crust | Non-crust | Total | |
| 1 | Crust | 16.2 | 2290 | 18 | 2308 | Training |
| 2 | Non-crust | 12.8 | 89 | 1242 | 1331 | Training |
| 3 | Mixed | 10.8 | 1096 | 1181 | 2277 | Verification |

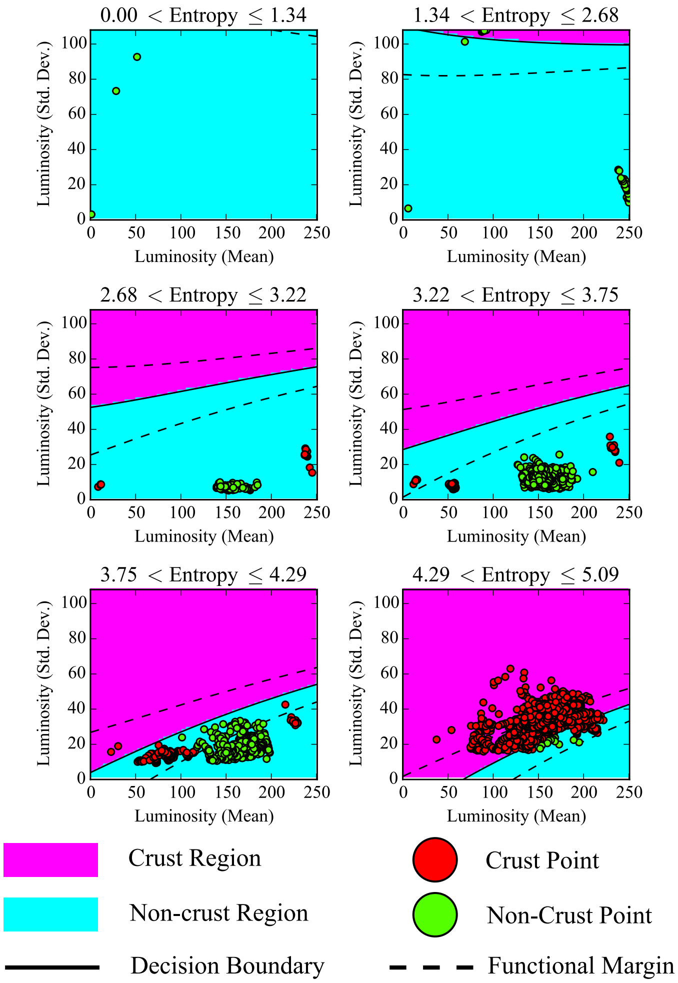


Fig. 4. The classification decision function generated by the SVM w.r.t. the parameters entropy and luminosity. The circles show the classified values of Patch 3. The lines show the decision curve at the upper limit of entropy.

to verify the proposed method. Transects along Takuyo No.5 seamount, which is located in the Pacific ocean, were scanned using the aforementioned systems mounted on ROV Hyper-Dolphin, at depths between 1400 and 1700 metres. The data was collected, stored and processed offline.

From the pre-processed 3D map output of the visual mapping instrument, three areas are selected for initial analysis. These are listed in table I. The visual and acoustic data are processed for each of the patches as described in the previous section.

For the task of training the SVM classifier, two patches are selected - one containing continuous deposits of crust and one with sediment deposits on top. These two patches are shown in fig. 3. The line on top shows the trace of acoustic beam on the seafloor. The colour of the line denotes the type of seafloor

TABLE II. CLASSIFICATION RESULTS - CONFUSION MATRIX

| Patch 1 | | Detected Type | | | Accuracy (%) |
|---|---|---|---|---|---|
| | | Crust | Non-crust | Total No. | |
| Actual Type | Crust | 2265 | 66 | 2331 | 97.2 |
| | Non-crust | 59 | 70 | 129 | 54.3 |
| Total No. | | 2324 | 136 | 2460 | 94.9 |
| **Patch 2** | | **Detected Type** | | | **Accuracy (%)** |
| | | Crust | Non-crust | Total No. | |
| Actual Type | Crust | 8 | 19 | 27 | 29.6 |
| | Non-crust | 12 | 1420 | 1432 | 99.2 |
| Total No. | | 58 | 1273 | 1331 | 97.9 |
| **Patch 3** | | **Detected Type** | | | **Accuracy (%)** |
| | | Crust | Non-crust | Total No. | |
| Actual Type | Crust | 898 | 198 | 1096 | 81.9 |
| | Non-crust | 135 | 1046 | 1181 | 88.6 |
| Total No. | | 1033 | 1244 | 2277 | 85.4 |

predicted by the algorithm, after training, with green indicating crust and red showing everything else. The authors used SVC class of the scikit-learn library package for python (based on libsvm) for the processing [4]. The trained classifier model is shown in fig. 4.

The model was validated on all the three patches previously selected. The patches were checked manually to distinguish CRC from non-CRC regions. This information was then compared with the prediction by the SVM model. The two patches used for training was used to test self-consistency; the patches and the predicted type of seafloor are shown in fig. 3. The results are tabulated and is shown in table II. More than 90% percent of the discs were correctly identified by the classifier.

The third patch, which contains both types of seafloor, and its prediction by the classifier is shown in detail in fig 5. The first figure shows the pre-processed output of the visual system, i.e, the 3D colour map. The prediction by the SVM classifier is overlaid on it. The green dots denote the presence of crust and the red dots denote the absence of crust. After discarding the thickness measurements where crust is not present, the final figure is obtained. It shows the 3D-map overlaid with the thickness values as a colour coded 3D bar chart, where both the colour and the height of each bar represents the thickness. The test data is also plotted in fig. 4. As shown in table II, comparing with the manually classified data, 85.4% of the discs were recognized successfully.

## V. DISCUSSION

This paper describes a method to filter and validate acoustic thickness measurement based on visual information of the same region. An overview of the system and key parts of the algorithm are presented. The results show a high accuracy of 85.4%, with an untrained dataset. This serves as an effective tool to filter acoustic data and leave only relevant measurements of crust in areas with complex distribution of crust, without depending on the acoustic data. Further work on the topic will focus on testing the generality of the method by expanding the test data and verifying performance, and then applying it to estimate the volumetric distribution of crust at the surveyed seamount.

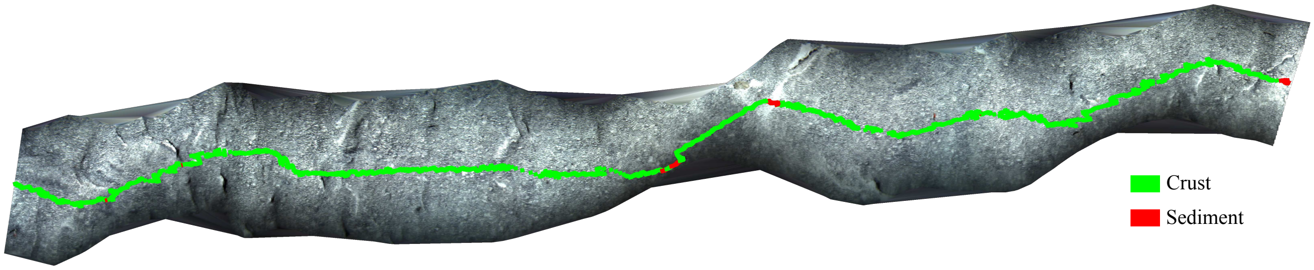


(a) Training data consisting mostly of crust (Patch 1)

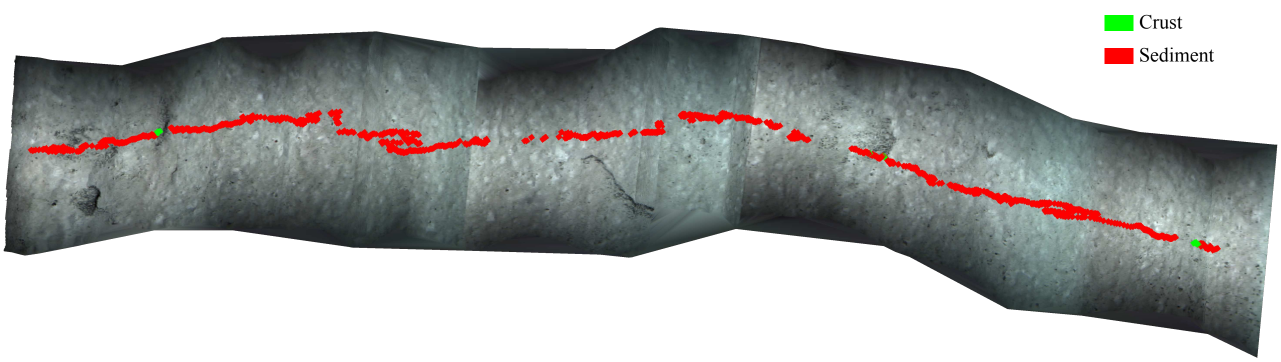


(b) Training data consisting mostly of sediment (Patch 2)

Fig. 3. Patches used for training the SVM model overlaid with predicted type

## Acknowledgment

The authors would like to thank the Hyper-Dolphin team and R/V Natsushima crew, Japan Agency for Marine-Earth Science and Technology (JAMSTEC) during the NT13-13 cruise. This work was supported by the Japanese Ministry of Education under the Program for the Development of Fundamental Tools for the Utilization of Marine Resources.

## References

[1] A. Usui, I. J. Graham, R. G. Ditchburn, A. Zondervan, H. Shibasaki, and H. Hishida, "Growth history and formation environments of ferromanganese deposits on the philippine sea plate, northwest pacific ocean," *Island Arc*, vol. 16, no. 3, pp. 420–430, 2007.

[2] B. Thornton, A. Asada, A. Bodenmann, M. Sangekar, and T. Ura, "Instruments and Methods for Acoustic and Visual Survey of Manganese Crusts," *IEEE Journal of Oceanic Engineering*, vol. 38, no. 1, pp. 186–203, January 2013.

[3] A. Bodenmann, B. Thornton, and T. Ura, "3D Seafoor Mapping With Automated Data Analysis," *Sea Technology*, pp. 41–46, October 2012.

[4] F. Pedregosa, G. Varoquaux, A. Gramfort, V. Michel, B. Thirion, O. Grisel, M. Blondel, P. Prettenhofer, R. Weiss, V. Dubourg, J. Vanderplas, A. Passos, D. Cournapeau, M. Brucher, M. Perrot, and E. Duchesnay, "Scikit-learn: Machine learning in Python," *Journal of Machine Learning Research*, vol. 12, pp. 2825–2830, 2011.

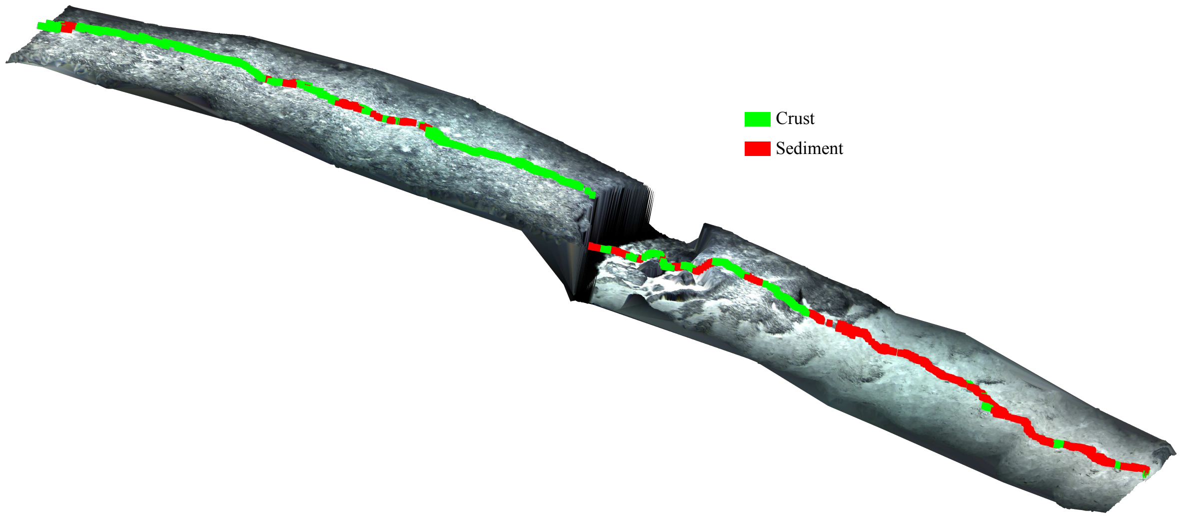


(a) Test data showing predicted type of seafloor determined by the classifier (85.4% accuracy)

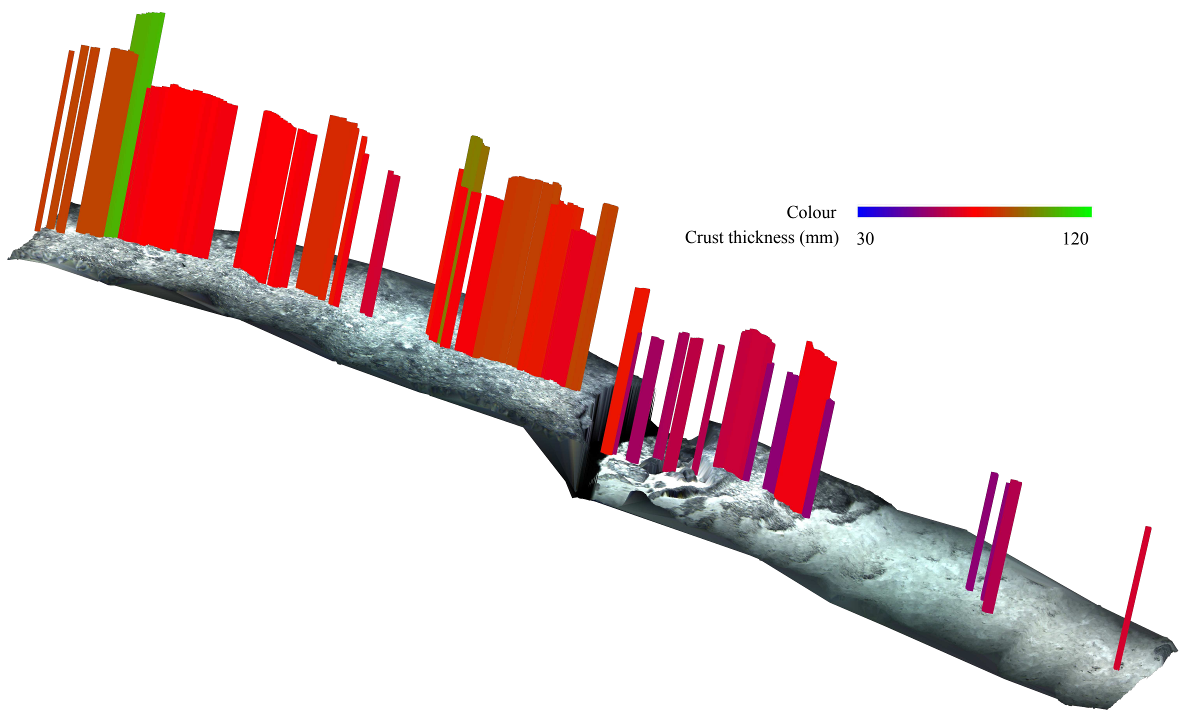


(b) Test data showing relevant crust thickness measurements overlaid

Fig. 5. Combined visual and acoustic outputs using proposed algorithm for test data